Temperatures on Europa from Galileo Photopolarimeter-Radiometer: Nighttime Thermal Anomalies

John R. Spencer,[1]* Leslie K. Tamppari,[2] Terry Z. Martin,[2] Larry D. Travis[3]

Galileo observations of Europa's thermal emission show low-latitude diurnal brightness temperatures in the range of 86 to 132 kelvin. Nighttime temperatures form an unexpected pattern, with high temperatures on the bright ejecta blanket of the crater Pwyll and an equatorial minimum in temperatures after sunset, uncorrelated with surface albedo or geology. The nighttime anomalies may be due to regional thermal inertia variations of an unknown origin, which are equivalent to a two- to threefold variation in thermal conductivity, or to endogenic heat fluxes locally reaching 1 watt per square meter. Endogenic heat flow at this high level, although consistent with some geological evidence, is theoretically unlikely.

Ice-covered Europa is one of the most remarkable of the four Galilean satellites of Jupiter. Its surface, perhaps still geologically active, is dominated by ridges and chaotic terrain, which suggest a rigid crust that is up to several kilometers thick and overlying soft warm ice or liquid water (*1*). Surface temperatures, which are determined by diurnal heat flow within the top few centimeters of the surface and are sensitive to surface composition and morphology (for example, porosity and grain size and shape), can cast light on the various processes [impact gardening, erosion (sputtering) by jovian magnetospheric ions (*2*), insolation-controlled sublimation (*3, 4*), or endogenic processes] that shape Europa's uppermost surface. The best Voyager thermal measurements (*5*) had limited coverage and low spatial resolution (900 km).

The photopolarimeter-radiometer (PPR) (*6, 7*), on the Jupiter-orbiting Galileo spacecraft has mapped thermal radiation from Europa's surface with a spatial resolution of 80 to 200 km. Pointing errors are smaller than the spatial resolution. Near-blackbody radiation is expected from the surfaces of the icy Galilean satellites because of the high opacity of water ice (*8*), and Voyager thermal emission spectra of Europa were consistent with gray body emission with a mean emissivity ε near 0.9 (*5*). Kinetic temperatures are slightly higher than the infrared brightness temperatures reported here, because $\varepsilon < 1$ (*9*). Observations presented here (Figs. 1 and 2), with noise levels <1 K, were obtained during the day on orbits E6 (20 February 1997) and G7 (5 April 1997) at a wavelength of 27.5 μm and at night on orbit E17 (26 September 1998), with a wide-open filter position sensitive to all radiation from 0.35 to ~100 μm (*10*).

Daytime brightness temperatures peak near 132 K for longitude 180°W (Fig. 1), consistent with ground-based disk-integrated radiometry (*11, 12*). Diurnal temperature variations (Fig. 2) constrain the surface bolometric albedo A and the effective thermal inertia Γ_e. If sunlight is absorbed at the surface, Γ_e is equal to the thermal inertia Γ, which is given by $\Gamma = \sqrt{(k\rho c)}$, where k is the surface thermal conductivity, ρ is the density, and c is the specific heat. Increasing Γ will increase nighttime temperatures. For a particulate surface, Γ variations tend to be dominated by variations in k, because of variations in compaction, grain size, or effectiveness of grain-to-grain heat flow (*13*), although composition may also be important. In icy materials, however, sunlight may be absorbed below the surface (*14*), which also increases nighttime temperatures. Thermal inertia and sunlight penetration effects are difficult to distinguish on the basis of surface temperature measurements (*15*), and Γ_e as defined here may include contributions from Γ and from sunlight penetration. Because data from different times of the day come from different parts of the surface, Fig. 2 provides only an approximation to the diurnal temperature variation of any particular place on Europa's surface but gives some constraint on global A and Γ_e values. Assuming $\varepsilon = 0.9$, a homogeneous thermal model with $A = 0.55$ and $\Gamma = 7 \times 10^4$ erg cm^{-2} s$^{-1/2}$ K^{-1} [20 times lower than the value for solid ice and thus indicating a particulate surface, as also indicated by photometric and eclipse cooling studies (*11, 16*)] produces about the observed diurnal brightness temperature range but is clearly a poor fit to the data, which are more symmetrical around midday than the temperatures shown by the model. The difference may be largely because existing prenoon observations cover the darker and warmer trailing hemisphere of Europa (*11, 12*). However, unresolved vertical or lateral Γ_e inhomogeneities, required by eclipse observations of the icy Galilean satellites (*5, 11*), would also make the diurnal thermal profile more symmetrical (*6*). Our best fit model has a bolometric albedo A, consistent with the photometrically derived value of 0.62 ± 0.14 (*17*), and gives an equatorial diurnal and seasonal mean surface temperature (an important boundary condition for interior models) of 106 K.

Local daytime brightness temperatures correlate inversely with albedo, as expected from equilibrium with absorbed sunlight (Fig. 1). On a global scale, the same is true at night. Longitudes 0° through 75°W, seen after sunset (*18*), with a typical 0.48-μm normal albedo of 0.65 (*19*), are generally colder than longitudes 240° through 300°W, seen before dawn, where the typical albedo is 0.5. However, much of the smaller scale nighttime temperature variability does not follow the expected darker = warmer rule. For example, peak predawn brightness temperatures (95 K near 15°S, 280°W) include the bright ejecta blanket of the crater Pwyll (26°S, 271°W). Most remarkable is the systematic variation with latitude of the postsunset temperatures: Northern latitudes are warmer than equivalent southern latitudes, and there is a temperature minimum along the equator. At longitude 55°W, brightness temperatures are 94.5, 88.0, and 90.5 K at 30°N, 2°S, and 30°S, respectively. Voyager 0.48-μm images of these longitudes show a global-scale trend of increasing albedo away from the equator (*19*), perhaps related to the thermal pattern, although in the opposite sense to the expected trend if temperature was controlled directly by albedo (*20*). However, the Voyager images and the best Galileo images of this longitude range (with a resolution of 12 km per pixel, used as the base map in Fig. 1) also show albedo patterns on a 200-km scale that are comparable in magnitude to the equator-to-pole variations and are not reflected in the PPR temperature distribution.

Emissivity variations are unlikely to produce the observed large variations in broadband thermal emission, as decreased emissivity will increase surface kinetic temperature by inhibiting radiative heat loss. Difficulties

[1]Lowell Observatory, 1400 West Mars Hill Road, Flagstaff, AZ 86001, USA. [2]Jet Propulsion Laboratory, 4800 Oak Grove Drive, Pasadena, CA 91109, USA. [3]Goddard Institute for Space Studies, 2880 Broadway, New York, NY 10025, USA.

*To whom correspondence should be addressed. E-mail: spencer@lowell.edu

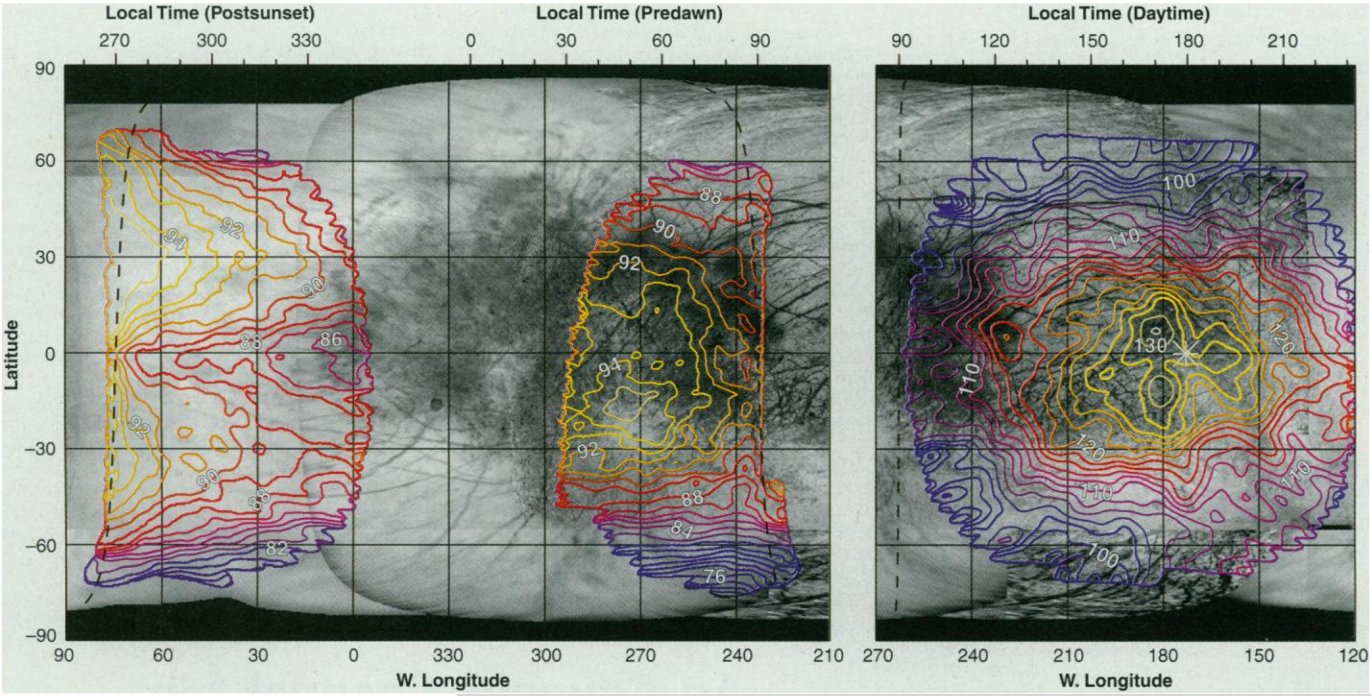

Fig. 1. Contours of brightness temperature distributions on Europa (nighttime from orbit E17 and daytime from orbit G7). Contour interval is 1 K for the nighttime map and 2 K for the daytime map, and contour color scheme is different for the two maps. Local time (top axis) is given in degrees of rotation after midnight, the terminator is shown by the black dashed lines, and the subsolar point is shown by a white star. Base map is from the best available Galileo and Voyager images (*33*).

with this and other alternative explanations of the observed nighttime temperature anomalies point to variation in Γ_e as the most likely cause. A change in Γ_e from 7×10^4 to 4.5×10^4 erg cm^{-2} s$^{-1/2}$ K^{-1} (produced, for instance, by a 2.4-fold drop in k) will reduce equatorial temperatures by 5 K at a local time 30° after sunset (Fig. 2), comparable to the magnitude of the observed thermal anomalies. The difficulty then lies in explaining the spatial patterns of Γ_e variation inferred from the observations. Higher Γ_e values near the crater Pwyll might result from an increased abundance of large regolith particles (of size comparable to or greater than the diurnal skin depth, which is 4 cm for our best fit model and an assumed regolith density of 0.5 g cm^{-3}) in the ejecta blanket or from 1 to 2 cm of sunlight penetration (*15*) in the ice-rich material of the ejecta. Lunar eclipse thermal data show a somewhat similar pattern of warm temperatures on crater ejecta blankets within 1 crater diameter of the rim, produced by the enhanced abundance of rocky blocks there (*21*), although the Pwyll anomaly is much larger (extending more than 250 km, 10 crater diameters, from the rim) and is not perfectly centered on the crater. The postsunset temperatures are even more problematic because they are correlated with latitude, but there is no observed correlation with underlying geology (*22*). A preliminary analysis of 1- to 2.5-μm spectra from the Galileo near-infrared mapping spectrometer (*23*) shows a trend of larger photon path lengths in ice at higher latitudes. This is consistent with the PPR postsunset temperature distribution if the larger path lengths result from increased contact between ice grains, which would increase k and thus Γ_e and thus nighttime temperature at high latitudes. However, simple theoretical considerations predict an opposite trend: The high daytime temperatures at low latitudes will tend to cause grain sintering (*24*), which will increase k and thus Γ_e at low latitudes. Large, sintered grains will allow greater sunlight penetration, which also tends to increase Γ_e. Surface texture could also be affected by the impact of jovian magnetospheric ions, but large gradients in ion flux with latitude in the 0° through 75°W region are not expected (*25*), especially as Galileo has ruled out an intrinsic magnetic field strong enough to deflect bombarding ions (*26*).

The most intriguing hypothesis is that the nighttime temperature anomalies are due to warming of the surface by endogenic heat conducted through the lithosphere. Tidal heating in an ice shell decoupled from the interior is predicted to be two to five times greater at the pole than at the equator (*27*), consistent with the cold equator seen in the postsunset temperature data. The local heat flow required to raise the surface temperature from 88.0 to 94.5 K is 1.1 W m^{-2}. For a crustal conductivity of 2.7 W m^{-1} K^{-1} (*28*), this would imply a thickness for the conductive lithosphere (between the mean surface temperature and near-melting temperatures) of only 0.34 km, within the range of Galileo-based estimates of lithospheric thickness [0.1 to 15 km (*29*)]. However, current models of Europa tidal heating predict a far smaller global mean heat flow [≤0.05 W m^{-2} (*27, 30*)], so an endogenic explanation of the thermal anomalies is probably unlikely.

The nighttime temperature observations can also be used to search for small, local, endogenic thermal anomalies ("hot spots") on

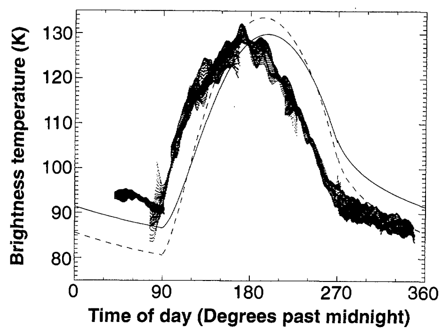

Fig. 2. Europa diurnal brightness temperature profile, combining data from Galileo orbits E6 and G7 (daytime) and E17 (nighttime). Only regions within 15° of the equator, seen at less than 65° from vertical, are included. Model diurnal temperature profiles for surfaces with $A = 0.55$ and $\Gamma = 7 \times 10^4$ erg cm^{-2} s$^{-1/2}$ K^{-1} (solid line) and $\Gamma = 4.5 \times 10^4$ erg cm^{-2} s$^{-1/2}$ K^{-1} (dashed line) are shown. The models were run separately for the different heliocentric distances and wavelengths of the daytime and nighttime data, resulting in small discontinuities at sunrise and sunset.

Europa, which might persist for decades after local geological activity has ceased (*31*). We have not detected any such endogenic hot spots. Upper limits to hot spot circular-equivalent diameter and temperature in the 18% of Europa's surface covered by our most sensitive observations (the low-latitude nighttime coverage shown in Fig. 1) are 16.8 km at 130 K, 6.2 km at 200 K, 3.4 km at 273 K, or 2.0 km at 350 K. This is much fainter than a brief thermal event tentatively identified in 1981 ground-based observations (*32*).

References and Notes

1. R. T. Pappalardo *et al.*, *J. Geophys. Res.*, in press; M. H. Carr *et al.*, *Nature* **391**, 363 (1998); R. Greeley *et al.*, *Icarus* **135**, 4 (1998).
2. W.-H. Ip *et al.*, *Geophys. Res. Lett.* **25**, 829 (1998).
3. J. R. Spencer, *Icarus* **69**, 297 (1987).
4. R. N. Clark, F. P. Fanale, A. P. Zent, *ibid.* **56**, 233 (1983).
5. J. R. Spencer, dissertation, University of Arizona, Tucson (1987).
6. In radiometric mode, PPR is a single-element bolometer with a circular field of view that is 2.5 mrad in diameter, which maps thermal emission from its targets by raster scanning of the Galileo scan platform on which it is mounted [E. E. Russell *et al.*, *Space Sci. Rev.* **60**, 531 (1992)]. Absolute calibration is provided by an on-board blackbody reference, prelaunch calibration, and observations of deep space and has errors that are currently $\leq$3 K. Problems with the filter wheel have limited the choice of filters on each orbit. The maps presented in Fig. 1 were produced by median-filtering the PPR observations to reduce radiation noise and then averaging all PPR observations whose fields of view overlap each point on the map.
7. G. S. Orton, J. R. Spencer, L. D. Travis, T. Z. Martin, L. K. Tamppari, *Science* **274**, 389 (1996).
8. S. G. Warren, *Appl. Opt.* **23**, 1206 (1984).
9. The brightness temperature of a body is the temperature of a blackbody with the same thermal emission brightness. For $\varepsilon = 0.9$, kinetic temperatures will be higher than broadband brightness temperatures by the factor $0.9^{-0.25}$, or 1.027.
10. The open filter is sensitive to Jupiter-shine reflected from Europa's nightside in addition to thermal radiation. Calculations based on daytime observations show that the Jupiter-shine contribution to apparent brightness temperatures will be <0.3 K before dawn and <1.0 K after sunset. Because albedo on scales of 100 km or larger varies by less than a factor of 2 on Europa, apparent local postsunset temperature variations due to local albedo variations will be <0.5 K. Tests using Voyager Europa spectra show that broadband and 27.5-μm brightness temperatures generally agree to $\leq$1 K.
11. D. Morrison, in *Planetary Satellites*, J. Burns, Ed. (Univ. of Arizona Press, Tucson, AZ, 1977), pp. 269–301. Thermal radiation varies considerably with longitude, peaking near longitude 270°.
12. D. L. Blaney, J. D. Goguen, G. J. Veeder, T. V. Johnson, D. L. Matson, *Lunar Planet. Sci.* **XXX** (CD-ROM, abstr. 1657)(1999).
13. A. E. Wechsler, P. E. Glaser, J. A. Fountain, in *Thermal Characteristics of the Moon*, J. W. Lucas, Ed. (MIT Press, Cambridge, MA, 1972), pp. 215–241.
14. R. H. Brown and D. Matson, *Icarus* **72**, 84 (1987).
15. M. L. Urquhart and B. M. Jakosky, *J. Geophys. Res.* **101**, 21169 (1996).
16. P. Helfenstein *et al.*, *Icarus* **135**, 41 (1998); D. L. Domingue, B. W. Hapke, G. W. Lockwood, D. T. Thomson, *ibid.* **90**, 30 (1991).
17. B. J. Buratti and J. Veverka, *ibid.* **55**, 93 (1983).
18. "Postsunset" observations cover a range of local time (measured in degrees of rotation after midnight) of 270° through 345°, from 0 to 18 hours after sunset. Similarly, "predawn" observations cover local times of 30° through 90°, from 14 to 0 hours before sunrise. At the equator, europan day and night each last 1.775 Earth days.
19. A. S. McEwen, *J. Geophys. Res.* **91**, 8077 (1986).
20. The Voyager images used by McEwen (*19*) at longitudes 0° through 75°W were taken at solar phase angles of 3° and 12° and do not show bolometric albedo, which accounts for light reflected in all directions. Variations in light-scattering properties at a high solar phase angle might produce variations in bolometric albedo that are not apparent in these images, but unrealistically large scattering variations would be required to reverse the trend of albedo with latitude, as would be required if albedo was the direct cause of the observed postsunset temperature variations.
21. J. M. Saari and R. W. Shorthill, *Icarus* **2**, 115 (1963); R. L. Wildey, B. C. Murray, J. A. Westphal, *J. Geophys. Res.* **72**, 3743 (1967).
22. The resolution (12 km per pixel) of the best Galileo images of this area is sufficient to distinguish major ridge systems and show the location of chaotic terrain, which is revealed by its low albedo and mottled appearance.
23. G. B. Hansen, personal communication.
24. J. Eluszkiewicz, *J. Geophys. Res.* **96**, 19217 (1991); R. B. Alley *et al.*, *J. Glaciol.* **32**, 415 (1986).
25. M. K. Pospieszalska and R. E. Johnson, *Icarus* **78**, 1 (1989).
26. M. G. Kivelson *et al.*, *Science* **276**, 1239 (1997).
27. G. W. Ojakangas and D. J. Stevenson, *Icarus* **81**, 220 (1989).
28. P. V. Hobbs, *Ice Physics* (Oxford Univ. Press, London, 1974).
29. K. K. Williams and R. Greeley, *Geophys. Res. Lett.* **25**, 4273 (1998); J. M. Moore *et al.*, *Icarus* **135**, 127 (1998).
30. S. W. Squyres *et al.*, *Nature* **301**, 225 (1983); M. N. Ross and G. Schubert, *ibid.* **325**, 133 (1987).
31. J. E. VanCleve, in preparation. For a surface heated only by sunlight, the maximum possible equatorial nighttime temperature (assuming zero albedo and infinite thermal inertia) is 130 K, and warmer nighttime temperatures would be an unambiguous sign of endogenic activity.
32. W. C. Tittemore and W. M. Sinton, *Icarus* **77**, 82 (1989). This event, if real and thermal in origin, implied a region with a diameter of 176 km at 273 K or a region of 52 km at 350 K.
33. C. Phillips, personal communication.

34. This work was supported by the Galileo project and NASA grant NAG5-6794. We thank L. Barnard and O. Liepack for assistance with design and implementation of the observation sequences and the entire Galileo team at the Jet Propulsion Laboratory for making the Galileo mission a success. The paper benefited from comments by R. Pappalardo, P. Geissler, and D. Domingue.

14 January 1999; accepted 14 April 1999

An Aqueous Channel for Filamentous Phage Export

Denise K. Marciano, Marjorie Russel,* Sanford M. Simon*

Filamentous phage f1 exits its *Escherichia coli* host without killing the bacterial cell. It has been proposed that f1 is secreted through the outer membrane via a phage-encoded channel protein, pIV. A functional pIV mutant was isolated that allowed *E. coli* to grow on large maltodextrins and rendered *E. coli* sensitive to large hydrophilic antibiotics that normally do not penetrate the outer membrane. In planar lipid bilayers, both mutant and wild-type pIV formed highly conductive channels with similar permeability characteristics but different gating properties: the probability of the wild-type channel being open was much less than that of the mutant channel. The high conductivity of pIV channels suggests a large-diameter pore, thus implicating pIV as the outer membrane phage-conducting channel.

The pIV protein is one of three filamentous phage proteins that are not part of the f1 virion but are required for phage export from the host bacterium. Interest in pIV has been stimulated by its sequence similarity to proteins in the type IV pilus assembly and in transport pathways, including type II and type III secretion systems (*1*). Both of these complex secretion systems mediate the export of proteins in Gram-negative bacteria. In type II secretion, toxins or degradative enzymes are secreted into the extracellular milieu; in type III secretion, proteins are secreted and injected directly into the cytosol of eukaryotic host cells, causing cytotoxicity. Bacteria with type II or type III secretion systems include such notorious animal and plant pathogens as *Yersinia*, *Salmonella*, *Shigella*, and *Erwinia*, all of which express a pIV homolog necessary for secretion or virulence. Although it has been postulated that pIV and its homologs function as outer membrane channels, there has been no direct evidence to support this hypothesis.

The pIV protein exists as a large homomultimer in the outer membrane of *E. coli*. Purified multimers are large cylindrical structures, as viewed by scanning transmission electron microscopy (STEM) (*2*). The filamentous phage is approximately 1 μm long with a diameter of 6 to 7 nm. A simple diffusion pore 6 to 7 nm in diameter would cause *E. coli* to be very sensitive to external stresses. However, phage-infected *E. coli* maintain long-term viability. Thus, if pIV were to form a channel, it would most likely be opened only during phage export by a gating mechanism.

The Rockefeller University, 1230 York Avenue, New York, NY 10021, USA.

*To whom correspondence should be addressed. E-mail: russelm@rockvax.rockefeller.edu (M.R) and simon@rockvax.rockefeller.edu (S.M.S.)